

## Title Page

# **KU675, a Concomitant Heat Shock Protein Inhibitor of Hsp90 and Hsc70 that Manifests Isoform Selectivity for Hsp90 $\alpha$ in Prostate Cancer Cells**

Weiya Liu, George A. Vielhauer, Jeffrey M. Holzbeierlein, Huiping Zhao, Suman Ghosh,  
Douglas Brown, Eugene Lee, and Brian S. J. Blagg

Department of Urology, University of Kansas Medical Center, Kansas City, Kansas (W.L.,  
G.A.V., J.M.H., D.B., E.L.)

Department of Medicinal Chemistry, University of Kansas, Lawrence, Kansas (H. Z., S. G.,  
B.S.J.B.)

## Running Title Page

### *Running Title*

KU675, C- terminal isoform selective inhibitor of Hsp90

### *Corresponding author*

Jeffrey M. Holzbeierlein, MD, FACS

Department of Urology

University of Kansas Medical Center

3901 Rainbow Blvd, Mailstop 3016

Kansas City, KS 66160

E-mail: [jholzbeierlein@kumc.edu](mailto:jholzbeierlein@kumc.edu)

### *Corresponding author*

Brian S. J. Blagg, PhD

Department of Medicinal Chemistry

University of Kansas

1251 Wescoe Hall Drive, Malott 4070

Lawrence, KS 66045

E-mail: [bblagg@ku.edu](mailto:bblagg@ku.edu)

*Number of Text Pages: 25*

*Number of Figures: 6*

*Number of Reference: 47*

*Words in Abstract: 240*

***Words in Introduction: 866***

***Words in Discussion: 904***

***List of Non-Standard Abbreviations:***

17-AAG: 17-allylamino-17-demethoxygeldanamycin

AR: androgen receptor

BN: blue native

DMSO: dimethyl sulfoxide

EDTA: ethylenediaminetetraacetic acid

FBS: fetal bovine serum

Hsp: heat shock protein

Hsp90 $\alpha$ : heat shock protein 90 alpha isoform

Hsp90 $\beta$ : heat shock protein 90 beta isoform

Hsc: heat shock cognate protein

HSR: heat shock response

MTS: 3-(4, 5-dimethylthiazol-2-yl)-5-(3-carboxymethoxyphenyl)-2-(4-sulfophenyl)- 2H-tetrazolium, inner salt

MEM: minimal essential media

NB: novobiocin

PBS: phosphate-buffered saline

## Abstract

The 90-kDa heat shock protein (Hsp90) assists in the proper folding of numerous mutated or overexpressed signal transduction proteins that are involved in cancer. Inhibiting Hsp90 consequently is an attractive strategy for cancer therapy as the concomitant degradation of multiple oncoproteins may lead to effective anti-neoplastic agents. Here we report a novel C-terminal Hsp90 inhibitor, designated KU675, which exhibits potent anti-proliferative and cytotoxic activity along with client protein degradation without induction of the heat shock response (HSR) in both androgen dependent and independent prostate cancer cell lines. In addition, KU675 demonstrates direct inhibition of Hsp90 complexes as measured by the inhibition of luciferase refolding in prostate cancer cells. In direct binding studies, the internal fluorescence signal of KU675 was utilized to determine the binding affinity of KU675 to recombinant Hsp90 $\alpha$ , Hsp90 $\beta$  and Hsc70 proteins. The  $K_d$  for Hsp90 $\alpha$  was determined to be 191  $\mu$ M while the  $K_d$  for Hsp90 $\beta$  was 726  $\mu$ M, demonstrating a preference for Hsp90 $\alpha$ . Western blot experiments with four different prostate cancer cell lines treated with KU675 supported this selectivity, by inducing the degradation of Hsp90 $\alpha$ -dependent client proteins. KU675 also displayed binding to Hsc70 with a  $K_d$  value at 76.3  $\mu$ M, which was supported in cellular by lower levels of Hsc70 specific client proteins upon western blot analyses. Overall, these findings suggest that KU675 is an Hsp90 C-terminal inhibitor as well as dual inhibitor of Hsc70, and may have potential use for the treatment of cancer.

## Introduction

Prostate cancer is the sixth leading cause of cancer-related death in men globally. In the United States, it is responsible for approximately 30,000 deaths annually, and ranks as the second leading cancer killer amongst men (Siegel et al., 2011). Prostate cancer tends to be detected in men over the age of fifty, and the treatments of patients with metastatic, locally recurrent, and androgen-independent prostate cancer are particularly problematic and often fatal. Huggins and Hodges reported the susceptibility of prostate tumors to undergo androgen withdrawal in 1952 (Huggins, 1952; Huggins and Hodges, 2002). Since then, patients with advanced prostate cancer have undergone treatment with therapies directed at inhibition of the androgen receptor (Lassi and Dawson, 2010). However, androgen withdrawal is not sufficient in the treatment of metastatic disease, as most patients eventually fail androgen-deprivation therapies. Although recent trials with docetaxel have demonstrated a reasonable survival advantage, the long term effectiveness of such chemotherapy remains limited (Chi et al., 2010; Kelly et al., 2012; Petrylak et al., 2004; Tannock et al., 2004). Hence, there remains a critical need for the development of novel therapies to treat advanced prostate cancer.

Heat shock protein 90 (Hsp90) represents one of the most promising biologic targets identified for the treatment of cancer. Hsp90 is commonly overexpressed in many cancer cells, including prostate cancer (Hanahan and Weinberg, 2000; Holzbeierlein et al., 2010; Isaacs et al., 2003). As a molecular chaperone, Hsp90 is responsible for the maturation of proteins directly associated with malignant progression, and therefore, inhibition of this protein folding

function results in a combinatorial attack on numerous pathways (Basso et al., 2002; Sato et al., 2000; Schulte and Neckers, 1998; Xu et al., 2001). Currently, many clinical trials for prostate cancer involve the targeting of proteins within the androgen receptor pathway, including kinases, growth factor receptors, or anti-apoptotic proteins. Notably, 75% of these drug targets are Hsp90-dependent client proteins (An et al., 2000; Blagosklonny et al., 1995; Schulte et al., 1995). Consequently, Hsp90-inhibition can target most of these pathways and provide a powerful new approach toward the treatment of prostate cancer.

Hsp90 exists as a dimer, and the binding of ATP to the N-terminal pocket of each monomer leads to formation of a “closed” formation that binds client proteins, facilitates folding, discourages protein aggregation, and mediates proteasomal degradation. A number of Hsp90 inhibitors that target the N-terminal ATP-binding pocket have demonstrated potent anti-proliferative effects (Avila et al., 2006; Roe et al., 1999; Whitesell and Lindquist, 2005), however, a major drawback associated with their use is that they induce a pro-survival heat shock response (HSR), which results in increased levels of Hsp27, Hsp40, Hsp70, and Hsp90 at the same concentration that leads to client protein degradation (Chiosis et al., 2003; Powers and Workman, 2007). Consequently, scheduling and dosing of these drugs is difficult and has limited their potential use. Compared to N-terminal inhibitors, the antibiotic, Novobiocin (NB), binds the C-terminus of Hsp90 and through Hsp90 C-terminal inhibitions, induces client protein degradation without induction of the pro-survival, heat shock response (HSR) (Burlison et al., 2008; Eskew et al., 2011; Matthews et al., 2010; Shelton et al., 2009). We have previously

reported the synthesis and evaluation of NB analogues that exhibit improved potency over NB (Eskew et al., 2011; Kusuma et al., 2014; Matthews et al., 2010; Shelton et al., 2009). In this manuscript, we report a new C-terminal inhibitor, KU675, which exhibits potent anti-proliferative effects in prostate cancer cells and a preference for the inhibition of Hsp90 $\alpha$ .

In mammalian cells, there are two Hsp90 isomers in the cytosol (Hsp90 $\alpha$  and Hsp90 $\beta$  in human). Additional Hsp90 homologues include Grp94 which is found in the endoplasmic reticulum, and Hsp75/TRAP1, in the mitochondrial matrix (Chen et al., 2006). There are two or more genes encoding cytosolic Hsp90 homologues, with the human Hsp90 $\alpha$  showing 85% identity to Hsp90 $\beta$  (Chen et al., 2005). Certain areas within the amino acid sequence that differ between Hsp90 $\alpha$  and Hsp90 $\beta$  raise the potential to exhibit isoform-specific functions, such as differential binding to client proteins (Sreedhar et al., 2004). These differences in function and expression of Hsp90 isoforms, provide the potential to develop isoform specific inhibitors of Hsp90 for antitumor therapies, which may have clinical importance (Csermely et al., 1998). Selective inhibition of individual Hsp90 isoforms may decrease toxicity, or, enhance potency depending on the pharmacology of the cancer. Unfortunately, most Hsp90 inhibitors undergoing clinical evaluation are pan-inhibitors, and bind all isoforms with similar affinity (Martin et al., 2008; Ohba et al., 2010; Stuhmer et al., 2009; Suda et al., 2014).

The aim of this study was to characterize the effects of the C-terminal Hsp90 inhibitor, KU675, a second generation analog of Novobiocin, in different prostate cancer cell lines. The results indicated that KU675 binds directly to Hsp90 and exhibits a robust anti-proliferative and



cytotoxic activity along with client protein degradation and disruption of Hsp90 native complexes without an induction of the heat shock response (HSR). KU675 also manifested some isoform selectivity for Hsp90 $\alpha$ , with a binding affinity three times higher than Hsp90 $\beta$ . In addition, KU675 also binds to Hsc70, and reduces the expression of Hsc70 specific client proteins. These findings reveal a novel direction for the design and synthesis of future C-terminal Hsp90 inhibitors.

## Materials and Methods

KU675 was synthesized as previously described (Burlison et al., 2008) (Fig. 1A). KU675, KU174, Novobiocin, and 17-AAG were dissolved in DMSO and stored at -80°C until use. Hsc70 recombinant protein was purchased from Stress Marq Biosciences Inc., Victoria, BC, Canada. The antibodies used for Western blot analysis included rabbit anti-Her2/ErB2 (#2165S), rabbit anti-Akt (#4691S), mouse anti-survivin (#2808S), rabbit anti-cdc25C (#4688S), mouse anti-Hsp27 (#2402S), rabbit anti-Hsf-1 (#4356S), rabbit anti- $\beta$ -actin (#4967L), rabbit anti-Cyclin D1 (#2922) (Cell Signaling Technologies, Danvers, MA), rabbit anti-B-Raf (#07-583) (Upstate Cell Signaling Solutions, Lake Placid, NY), rabbit anti-Hsc70 (#SPA-816), rat anti-Hsp90 $\alpha$  (#SPA-840) (Assay designs, Ann Arbor, MI), goat anti-Hsp90 $\beta$  (#SC-1057), mouse anti-AR (#SC-7305), mouse anti-Sp1 (#SC-420), mouse anti-c-Src (#SC-8056) (Santa Cruz Biotechnology, Inc., Santa Cruz, CA), rabbit anti-CXCR4 (#ab2074), rabbit anti-pAkt (S473) (#ab18206), rabbit anti-pAkt (T308) (#ab66134), rabbit anti-ERK5 (#ab40809) (Abcam Inc., Cambridge, MA), mouse anti-Nestin (#MAB5326), and mouse anti-Myb (#05-175) (Millipore Corporation, Temecula, CA).

### Hsp90 $\alpha$ and Hsp90 $\beta$ recombinant proteins

Overexpression and purification of Hsp90 $\alpha$  and Hsp90 $\beta$  were carried out in the vector pTBSG1 (Qin et al., 2008) by the Center of Biomedical Research Excellence in Protein Structure and Function, The University of Kansas, Lawrence, KS. Hsp90 $\alpha$  and  $\beta$  recombinant

proteins were further purified by AKTA Xpress purification system (GE Healthcare), aliquoted, and stored at  $-80^{\circ}\text{C}$  before use.

## Cell culture

PC3MM2 (androgen independent) and LNCaP-LN3 (androgen dependent) prostate cancer cell lines (Pettaway et al., 1996) were obtained from M.D. Anderson Cancer Center (Houston, TX) and cultured in MEM Eagle Medium (Sigma-Aldrich, St. Louis, MO) with 10% fetal bovine serum (FBS), penicillin/streptomycin (100 IU/ml/100 mg/ml), MEM vitamins, and MEM nonessential amino acid. LAPC-4 (androgen dependent) and C4-2 (androgen dependent) prostate cancer cell lines were kindly provided by Dr. Benyi Li (Department of Urology, The University of Kansas Cancer Center). LAPC-4 and C4-2 cells were cultured in Iscove's Modified Dulbecco's Medium (Sigma-Aldrich, St. Louis, MO) and RPMI 1640 Medium (Invitrogen, Carlsbad, CA), respectively, supplemented with 10% FBS and penicillin/streptomycin (100 IU/ml/100 mg/ml). All cells were maintained at  $37^{\circ}\text{C}$  with 5%  $\text{CO}_2$ . The stably, transduced Hsp90 $\alpha$  and Hsp90 $\beta$  knockdown PC3MM2 cells were cultured as above but with the addition of 2.5  $\mu\text{g}/\text{mL}$  puromycin. The shRNA expression of Hsp90 $\alpha$  was induced with the addition of 12 or 24  $\mu\text{g}/\text{ml}$  doxycycline. Induction of Hsp90 $\alpha$  shRNA expression with tetracycline was monitored by the TurboRFP fluorescence. The Hsp90 $\beta$  shRNA was constitutively expressed and was monitored by TurboGFP fluorescent cells. Freeze down stocks of the original characterized cell-line were stored under liquid nitrogen. All experiments

were performed using cells with a passage number under 20 and less than three months in continuous culture.

### **Anti-Proliferative Assay**

Cellular viability was assessed using the Cell Titer-Glo<sup>®</sup> Luminescent Cell Viability Assay (Promega, Madison, WI) according to the manufacturer's instructions. This approach is a homogeneous method to determine the number of viable cells in culture based on quantitation of the ATP present, which signals the presence of metabolically active cells. Briefly,  $5 \times 10^3$  cells/well were cultured in 96-well white plates in medium for 24h, then, incubated with KU675 for 24 and 48h time points. Luminescent signals were measured on the BioTek Synergy 4 Plate Reader (BioTek Instruments, Winooski, Vermont). Data were analyzed from three independent experiments performed in triplicate, and non-linear regression and sigmoidal dose-response curves (GraphPad Prism 5.0, La Jolla, CA) were used to calculate IC<sub>50</sub> and R<sup>2</sup> values.

### **Trypan blue cytotoxicity experiments**

Cell viability was conducted as previously described (Matthews et al., 2010). Prostate cancer cells were treated with KU675 for the indicated time points, and at the end of the incubation time for each cell treatment group, non-adherent cells were collected and combined with cells detached by trypsinization using TrypLE<sup>™</sup> Express (Invitrogen, Carlsbad, CA) followed by centrifugation at  $200 \times g$  at 4°C. Cell pellet was then re-suspended and washed twice with cold DPBS (Invitrogen, Carlsbad). Total cell counts and viability were conducted on

an automated system Vi-Cell™ Cell Viability Analyzer (Beckman Coulter Inc., Brea, CA). Data were statistically analyzed using a two-tailed t-test (GraphPad Prism 5.0, La Jolla, CA), all data displayed represent the mean  $\pm$  SEM from three independent experiments (n=3), asterisks \*, \*\*, and \*\*\* indicates significant *p* value  $< 0.05$ ,  $< 0.01$ , and  $< 0.001$  respectively, compared to vehicle-treated (DMSO) control.

### Western blot analysis

PC3MM2, LNCaP-LN3, LAPC-4 and C4-2 cells were seeded at a density of  $1.0 \times 10^6$  in T75 flasks. After 24 hours, the t=0 flask was harvested and cell number was counted by Vi-Cell as described above. Remaining flasks were dosed with drugs by serial dilution from DMSO stocks. Total cells after 24 hours of KU675 treatment were pelleted and suspended into PBS. Suspended cells were aliquoted for Vi-Cell viability measurements, total protein SDS-PAGE analysis and Blue-native (BN) electrophoresis. SDS-PAGE lysates were prepared in RIPA buffer: 50 mM Tris-HCl pH 7.5, 150 mM NaCl, containing 0.1% SDS, 1% Igepal, 1% sodium deoxycholate, protease, and phosphatase inhibitor cocktail (Sigma-Aldrich, Inc., St. Louis, MO), and lysed by three freeze-thaw cycles using liquid nitrogen and a 37°C water bath. Protein concentration was determined using DC Protein Assay (Bio-Rad Laboratories, Hercules, CA). Equal amounts of protein (20  $\mu$ g) were loaded on a Novex E-PAGE™ 8% protein gel (Life Technologies), transferred to a nitrocellulose membrane by Novex iBlot® Gel Transfer system (Invitrogen, Carlsbad, CA), blocked in TBS-T containing 5% milk, and probed with primary antibodies (1:1000 dilution). Membranes were incubated with IRDye® fluorescent

secondary antibody (1; 10,000 dilution), and visualized with the Odyssey Infrared Imager system (Li-cor, Lincoln, NE). All Western blots were probed for the loading control  $\beta$ -actin. The data were representative of at least three independent experiments (n=3).

### **Blue native (BN) gel electrophoresis**

After 24h of KU675 treatment, BN lysates were prepared from PC3MM2 cells in 20 mM Bis-Tris (pH7.4), 125 mM caproic acid, 20 mM KCl, 2mM EDTA, 5 mM MgCl<sub>2</sub>, 10% glycerol and 2% n-dodecyl beta-D-maltoside (DDM) followed by three freezing and thawing cycles and centrifugation at 14,000 g for 30 min at 4°C. Protein concentration was determined as described above and equal amounts of protein loaded on a Native PAGE Novex 3-12% Bis-tris gel (Invitrogen, Carlsbad, CA) and electrophoresed according to manufacturer's instructions. Membranes were incubated with a horseradish peroxidase-conjugated secondary antibody (1; 40,000 dilution), developed with chemiluminescence substrate (Pierce Biotechnology, Rockford, IL), and visualized with the UVP AutoChemi system (UVP, LLC, Upland, CA). A loading control  $\beta$ -actin was included in each experiment.

### **Cancer cell based Hsp90 dependent luciferase refolding assay**

The utilization of a reporter enzyme, such as luciferase, for the study of heat shock and related stress has been well established in our lab(Sadikot et al., 2013). Luciferase can be reversibly denatured, and its recovery is an active process mediated by the heat-shock proteins. The luciferase refolding assay was performed in PC3MM2 and LNCap-LN3 cells that have

been previously stably transfected with lenti virus carrying Luc2/mcherry genes. Cell pellets were collected from 80-90% confluent flasks and re-suspended in pre-warmed media (50°C) for approximately 5 minutes. Previous experiments have demonstrated that this is sufficient to denature the endogenous luciferase to less than 2% of the basal activity, but is insufficient to decrease viability of the cells. Cells were then plated at a density of 50,000 cells/well in a 96-well white plate in the presence of inhibitors. After one hour, the extent of refolded luciferase was measured by the addition of an equal volume of luciferase substrate solution and read on a Synergy<sup>TM</sup> 4 Multi-Detection Microplate Reader (BioTek Instruments Inc., Winooski, Vermont) set for 0.1 sec/well integration. Direct inhibition of luciferase was analyzed for each compound as previously described (Sadikot et al., 2013). EC<sub>50</sub> values were calculated from raw data plotted or normalized to a percentage control using a non-linear regression and sigmoidal dose response curves (GraphPad Prism 5.0, La Jolla, CA).

### **Intrinsic fluorescence spectroscopy**

Intrinsic fluorescence measurements were performed with a SpectraMax M5 Spectrophotometer (Molecular Devices Corporation, Sunnyvale, CA). KU675 was diluted to 20  $\mu$ M in assay buffer containing 20 mM HEPES, pH 7.4 and 50 mM NaCl. Recombinant Hsp90 $\alpha$ , Hsp90 $\beta$ , and Hsc70 proteins were added to the KU675 solution, adjusted to designed concentration (0 to 100  $\mu$ g/mL for Hsp90 $\alpha$ , 0 to 140  $\mu$ g/mL for Hsp90 $\beta$ , and 0 to 30  $\mu$ g/mL for Hsc70 recombinant proteins), and the mixture was allowed to incubate for 30 minutes before measurement. All measurements were made at 25°C and done in triplicate. The excitation

wavelength was 345 nm, and the emission was monitored from 350 nm to 600 nm. The concentration dependent binding curves were analyzed using non-linear fitting by GraphPad Prism 5 software (La Jolla, CA), and the affinity of binding ( $K_d$ ) were determined accordingly.



## Results

### Anti-proliferative effects of KU675 in prostate cancer cells

The anti-proliferative effects of KU675 were examined over a 48-hour time course against PC3MM2, LNCap-LN3, LAPC-4, and C4-2 prostate cancer cells (Fig. 1B-E). Prostate cancer cells were incubated with an increasing concentration of KU675 for 24 and 48 hrs, after which, cell viability was determined by Cell Titer-Glo® Luminescent Cell Viability Assay. As illustrated in Fig. 1, KU675 inhibited cell proliferation against PC3MM2 cells (androgen independent) in both a concentration- and time-dependent manner. For PC3MM2 cells, the  $IC_{50}$  values for KU675 were determined to be 7.5 and 4.4  $\mu$ M for 24 and 48 hr time points, respectively. Consistent with previous data, KU675 required longer treatment to achieve superior efficacy against the androgen independent PC3MM2 cell line as one might expect. However, for LNCap-LN3, LAPC-4, and C4-2 cells, the  $IC_{50}$  values for KU675 were determined to be 2.3, 1.7, and 1.6  $\mu$ M for 24 hr treatment, and 2.0, 1.6, 1.1  $\mu$ M for 48 hr treatment respectively, thus, the maximal potency of KU675 was essentially achieved at 24 hr for those three androgen dependent prostate cancer cells. In particular, compared to previous studies (Matthews et al., 2010), at our 24 hr time point, KU675 was 290-fold and 77-fold more potent ( $IC_{50}$ ) compared to the parent compound, novobiocin (NB), against the LNCap-LN3 and PC3MM2 cell lines, respectively. These findings indicate that, compared to novobiocin, KU675 possesses potent anti-proliferative activity against both androgen dependent and independent prostate cancer cell lines. As the androgen receptor (AR) is a client protein of Hsp90, and

LNCaP-LN3, LAPC-4, and C4-2 cells all contain a functional AR, it is not surprising that there is greater potency against those three cancer cell lines than the AR-deficient, PC3MM2 cell line.

### **Cytotoxicity of KU675 in prostate cancer cells**

Prostate cancer cells were further examined to discern the relationship between anti-proliferative effects and cytotoxicity. LNCap-LN3 (Fig. 2A), LAPC-4 (Fig. 2B), and C4-2 (Fig. 2C) cells were treated with KU675 for 24 hr, while PC3MM2 cells were treated for both 24 hr (Fig. 2D) and 48 hr (Fig. 2E). A dose-dependent increase in cell death was observed at concentrations of KU675 ranging from 0.5 to 10  $\mu$ M in LNCap-LN3 cells, 1.0 to 5.0  $\mu$ M in LAPC-4 cells, 0.5 to 5.0  $\mu$ M in C4-2 cells, and 5.0 to 25.0  $\mu$ M in PC3MM2 cells over 24 hr treatment. Comparing the total cell number upon KU675 treatment at each dose to time zero (right panels in Fig.2), revealed that 10  $\mu$ M KU675 is as cytostatic as 250  $\mu$ M novobiocin for LNCap-LN3 cells, 5  $\mu$ M for LAPC4 cells, 2.5  $\mu$ M for C4-2 cells, and 5  $\mu$ M for PC3MM2. With respect to cytotoxicity, KU675 appears more potent in androgen-dependent prostate cancer cells than androgen independent cancer cells, for example, 10  $\mu$ M KU675 is almost completely cytotoxic to LNCap-LN3 cells (Fig. 2A, left panel), while 25  $\mu$ M KU675 was necessary to kill most of the PC3MM2 cells (Fig. 2D, left panel). Additionally, PC3MM2 cells dosed with KU675 were further investigated at a 48 hr time point (Fig. 2E), since the antiproliferative results suggested KU675 might require longer exposure to elicit the maximal response for the PC3MM2 cell line (Fig. 1). At the 48 hr time point, KU675 demonstrated

appreciable cytotoxicity at doses as low as 5  $\mu$ M (Fig. 2E) in PC3MM3 cells, which not only correlated well with previous antiproliferative data, but also suggested that androgen independent cancer cells such as PC3MM2 might require higher dose and longer treatment to achieve the optimal result.

### **Cancer cell based Hsp90 dependent luciferase refolding assay**

Evidence suggests that Hsp90 is present in cancer cells as part of a large macromolecular complex, and therefore drugs that target Hsp90 activity should be engineered towards binding Hsp90 within physiologically relevant cancer cellular environment. Direct inhibition of the Hsp90 protein folding activity was assessed using a cancer-based luciferase refolding assay developed in our lab (Sadikot et al., 2013). The extent of luciferase refolding in the presence of the N-terminal inhibitor, 17-AAG, and the C-terminal inhibitor, KU675, was evaluated in both PC3MM2 (Fig. 3A) and LNCap-LN3 (Fig. 3B) cells. The N-terminal inhibitor, 17-AAG, was very potent with  $EC_{50}$  values in the low micro-molar range against both PC3MM2 and LNCap-LN3 cells (Fig. 3), in agreement with our prior studies. KU675, the C-terminal inhibitor, also showed significant inhibition, with similar  $EC_{50}$  values of  $\sim 50$   $\mu$ M for both PC3MM2 and LNCap-LN3 cells. Although KU675 exhibited a higher  $EC_{50}$  value than 17-AAG, after we normalized the data to percent control for comparison, we found, the maximum inhibition 17-AAG can achieve is  $\sim 50$  %, while KU675 can inhibit  $\square 80$  % (Fig. 3A-B). Overall, these data demonstrate that the luciferase refolding assay is a reliable method to determine on-target

Hsp90 inhibition in intact cancer cells, and that KU675 shows significant inhibition of Hsp90 activity in both androgen-dependent and -independent prostate cancer cells with over 80 % inhibition.

### **KU675 mediated degradation of client proteins**

The level of expression of Hsp90 client proteins has been shown to correlate with prostate cancer cell survival (Ayala et al., 2004; Isaacs et al., 2003; Kleeberger et al., 2007; Mohler, 2008; Zhang and Burrows, 2004), so the potential of KU675 to trigger degradation of client proteins, effect Hsp modulators, and its effect on heat shock protein induction were analyzed in both PC3MM2 (Fig. 4A), LNCap-LN3 (Fig. 4B), LAPC4 (Fig.4C), and C4-2 (Fig.4D) cells following 24 hours of treatment. In the PC3MM2 cell line, KU675 demonstrated a dose-dependent reduction in many Hsp90 client proteins such as Survivin, Akt, B-Raf, cdc25C, Her2/ErB2, and Nestin, whereas, no obvious changes were observed in the expression level of CXCR4. KU675 also significantly decreased the expression of Hsp modulators (Hsf-1) in PC3MM2 cells. In the LNCap-LN3, LAPC-4, and C4-2 cell lines, we also observed a dramatic degradation of several client proteins such as Survivin, Akt, cdc25C, Her2/ErB2, AR, and B-Raf without induction of the heat shock response. Different from the N-terminal inhibitor, 17-AAG, which causes a robust heat shock response and induction of Hsp27 and Hsc70 in all four prostate cancer cell lined tested (Fig. 4A-D), KU675 did not cause a heat shock response in PC3MM2. Moreover, KU675 demonstrated a modest dose-dependent reduction in Hsp's

(Hsc70 and Hsp27) in the LNCap-LN3, LAPC-4, and C4-2 cells (Fig. 4B-D), demonstrating again, that androgen-dependent prostate cancer cells are more sensitive to KU675 treatment. Interestingly, in all these prostate cancer cell lines, the expression level of CXCR4 remains unaffected. Additional studies with the Hsp90 $\alpha$  and Hsp90 $\beta$  knockdown cell lines (Peterson et al., 2012) revealed that, among many Hsp90 client proteins, Survivin, and B-raf are Hsp90 $\alpha$  specific client proteins, while CXCR4 is a client protein specifically dependent upon Hsp90 $\beta$  (Fig. 4E). Our client protein degradation data suggests that KU675 may possess Hsp90 isoform selectivity for Hsp90 $\alpha$ , since in four prostate cancer cell lines tested, we observed significant reduction of Hsp90 $\alpha$  client proteins, but the Hsp90 $\beta$  specific protein, CXCR4, remained unchanged.

### **Specific binding of KU675 to Hsp90 $\alpha$ / $\beta$ recombinant proteins**

The intensity of the KU675's intrinsic fluorescence spectra, as well as its maximum wavelength, are sensitive to the environments of the fluorescent side chain, thus, to determine the specific binding of KU675 to Hsp90, the interaction between KU675 and Hsp90 $\alpha$ / $\beta$  recombinant proteins was investigated by intrinsic fluorescent spectroscopy. When excited at 345nm, KU675 exhibits a fluorescence emission peak located at 450 nm, and the binding of KU675 to Hsp90 protein results in a small red shift of its fluorescence peak together with increased peak intensity. As can be seen in Fig. 5A and B (upper panels), in which the fluorescence emission peaks of KU675 are shown in the absence and presence of varying

concentrations of recombinant Hsp90 $\alpha$  and  $\beta$  proteins, Hsp90 causes around 5 nm red shift of KU675's maximum wavelength, and also enhances KU675's fluorescence peak intensity upon binding. As illustrated in the concentration-dependent binding curves (Fig. 5A and B, bottom panels), the binding of KU675 to Hsp90 was saturable with a calculated  $K_d$  of 191  $\mu$ M for Hsp90 $\alpha$  (Fig. 5A), and 726  $\mu$ M for Hsp90 $\beta$  (Fig. 5B). One negative control was also used in this study, phosphorylase kinase (PhK), which does not bind KU675, and as expected, only a slight fluorescence fluctuation was observed (Fig. 5C). Taken together, these results suggest that KU675 exhibits selective binding to Hsp90, and that the binding affinity for Hsp90 $\alpha$  is 3.8 times greater than Hsp90 $\beta$ , which corresponds well with the western blot data that show client protein degradations were Hsp90 $\alpha$  specific.

### **Analysis of native Hsp90 chaperone complexes by Blue Native-PAGE**

In order to further analyze KU675's binding selectivity for Hsp90 $\alpha$ , Blue Native-PAGE western blot was performed to assess disruption of the Hsp90 complex upon binding by KU675. Since Hsp90 functions as part of a large multiprotein complex, inhibition of Hsp90 leads to disruption of these complexes. These complexes resolve at a MW of 400 kDa for Hsp90 $\alpha$  and Hsp90 $\beta$ , and a lower MW of 150 kDa for Hsp90 $\alpha/\beta$  monomer/dimer (Fig. 5D). In blue native studies, differential disruption of Hsp90 $\alpha$  and Hsp90 $\beta$  complexes was observed upon binding to KU675. A robust disruption of Hsp90 $\alpha$  complex was observed with KU675's concentration as low as 1  $\mu$ M, for both Hsp90 $\alpha$  large complex and Hsp90 $\alpha$  monomer/dimer, while Hsp90 $\beta$  complex was

only moderately disrupted by KU675 at a concentration of 10  $\mu$ M. These observations, together with the previous western blot and binding affinity studies, further support KU675's ability to preferentially disrupt Hsp90 $\alpha$ .

### **Binding of KU675 to Hsc70 and the degradation of Hsc70's client proteins**

Further binding studies showed that KU675 also binds to Hsc70 protein, and that KU675 interacts with Hsc70 in a way different from its interaction with Hsp90 proteins. As shown in Fig. 6A, when Hsp90 was added to KU675, Hsp90 $\alpha$  and  $\beta$  enhanced KU675's fluorescence peak intensity with a small red shift for the peak position, however, addition of HSC70 led to a blue shift of KU675's fluorescence peak position along with an increase in peak intensity. Shifting of the peak toward a shorter wavelength indicates the fluorescent side chains of KU675 are buried in a less polar environment upon binding Hsc70, which is different from Hsp90. To further support that Hsc70 specifically binds to KU675, a protein titration was performed, and the concentration-dependent curve for the binding of KU675 to Hsc70 is shown in Fig. 6B. As illustrated in Fig. 6B, the binding of KU675 to Hsc70 was saturable with a calculated  $K_d$  of 76.3  $\mu$ M and a stoichiometry of 1 mol per mol of Hsc70. By comparison, Hsc70 exhibits a higher binding affinity for KU675 than Hsp90. Next, we tested the effect of KU675 binding to Hsc70 and its subsequent effect on Hsc70-dependent client proteins. Two Hsc70 client proteins, Myb

and Sp1, were chosen, and their expression and subsequent degradation were examined in the PC3MM2 and LNCap-LN3 cell lines exposed to KU675 for 24 hr. Degradation of the Hsc70 client proteins, Myb and Sp1, was observed in a dose-dependent manner in both cell lines (Fig. 6C), which again, strongly suggest that KU675 is a dual inhibitor of both Hsp90 and Hsc70 in prostate cancer cells.

## Discussion

Hsp90 is a molecular chaperone required for the folding of nascent and denatured proteins. Hsp90 is often present at elevated levels in cancer cells and it functions to stabilize oncogenic proteins involved in signal transduction, growth, and apoptosis regulation. There are approximately 200 reported cytosolic and nuclear client proteins of Hsp90, including protein kinases (e.g., Akt and Her2), transcription factors (e.g., mutant p53 and HIF-1 $\alpha$ ), chimeric signaling proteins, steroid receptors, and several proteins involved in apoptosis. Whereas many of the aforementioned Hsp90 client proteins are pursued individually as targets for anticancer drug development, inhibition of Hsp90 would prevent the maturation and stabilization of numerous Hsp90 client proteins simultaneously, leading to their degradation via the ubiquitin-proteasome pathway. Since 1995, when the first Hsp90 inhibitor was shown to demonstrate antitumor efficacy in a mouse xenograft tumor model, considerable efforts have focused upon



the development of Hsp90 inhibitors for the treatment of cancer. Although several N-terminal Hsp90 inhibitors, such as 17-AAG and its parent compound geldanamycin, have demonstrated client protein degradation, many of these agents have been hampered in clinical trials by high toxicity and/or poor solubility. A hallmark of N-terminal inhibition is induction of Hsps, which is mediated through HSF-1 transcriptional activation of the heat shock response element (HSE), and is a significant concern because clinical resistance has been attributed to the induction of these pro-survival Hsps. Efforts to increase the doses of the N-terminal inhibitors to overcome this resistance have been prevented due to toxicity, which may limit the clinical potential for these compounds.

A new approach to target Hsp90 began with the observation that the antibiotic, Novobiocin, binds with low affinity to a C-terminal ATP-binding pocket. (Marcu et al., 2000) Since then, more potent analogs of Novobiocin have been developed, and we report here one such candidate, KU675. This compound binds directly to Hsp90 and suppresses cell proliferation against androgen-dependent and -independent prostate cancer lines. In comparison to Novobiocin, KU675's antiproliferative effects were found to be 290-fold more potent against the LNCap-LN3 cells and 77-fold more against PC3MM2 cells (Fig. 1, 2). In a cancer cell-based Hsp90 dependent luciferase refolding assay, KU675 also exhibited greater inhibition of Hsp90's protein folding function than the N-terminal inhibitor, 17-AAG. The maximum inhibition achieved by 17-AAG was ~50 %, while KU675 suppressed the protein folding machinery  $\square$  80 % (Fig. 3). More importantly, KU675 in prostate cancer cells not only induced

the degradation of client proteins, but also caused concomitant reduction of Hsp27, Hsc70 and Hsf-1 (Supplemental Figure 1). The induction of a heat shock response, which was initially believed to be a hallmark of N-terminal Hsp90 inhibition, was not observed in either androgen-dependent LNCap-LN3, LAPC4, and C4-2 cells or androgen-independent PC3MM2 cells after KU675 treatment, which may have important clinical implications. The most interesting find in this study is that some Hsp90 $\alpha$  specific client proteins such as B-Raf and Survivin were affected across prostate cancer cell lines, however, the Hsp90 $\beta$  specific client protein, CXCR4, was minimally affected. The fact that not all client proteins would be equally degraded upon KU675 treatment suggests that KU675 may be selective for Hsp90 $\alpha$  inhibition.

In this study, for the first time, we revealed that the C-terminal Hsp90 inhibitor, KU675, exhibited preferential inhibition of Hsp90 $\alpha$ . KU675 appeared to have distinct effects on Hsp90 $\alpha$  specific client proteins such as B-Raf, and Survivin in all four prostate cancer cell lines we tested (Fig. 4), however, the level of the Hsp90 $\beta$ -dependent client protein, CXCR4, was minimally affected. Also, analysis of the binding of KU675 to Hsp90 by intrinsic fluorescent spectroscopy indicated that KU675 binds to Hsp90 preferentially with a  $K_d$  of 191  $\mu$ M for Hsp90 $\alpha$ , and a  $K_d$  of 726  $\mu$ M for Hsp90 $\beta$ . The binding affinity of KU675 for Hsp90 $\alpha$  is 3 times greater than its affinity for Hsp90 $\beta$  (Fig. 5). Finally, blue native western blots also showed that KU675 disrupts the Hsp90 $\alpha$  complex, including both the Hsp90 $\alpha$  monomer and dimer at 1  $\mu$ M, while only affecting the Hsp90 $\beta$  complex moderately at the same concentration. When combined, these data support the isoform selectivity of KU675 for Hsp90 $\alpha$ .

Furthermore, KU675 also displayed binding to Hsc70 with a  $K_d$  value of 76.3 $\mu$ M, and as a promising Hsc70 inhibitor, KU675, also decreased the levels of Hsc70 specific client proteins. The fact that KU675 is a dual inhibitor for both Hsp90 and Hsc70 was also supported by our luciferase refolding assay, in which the N-terminal inhibitor 17-AAG, a geldanamycin analog, only inhibited luciferase folding around 50%, but KU675 resulted in inhibition of over 80%. Research by Thulasiraman and Mattes's (Thulasiraman and Matts, 1996) demonstrated that geldanamycin did not inhibit luciferase folding by 100%, and that there was an alternate slower pathway through which luciferase could refold. This alternate pathway may represent an Hsp70-dependent pathway, since the study showed that direct Hsp70-inhibitors also block luciferase refolding (Thulasiraman and Matts, 1998). KU675 being a dual inhibitor would block both pathways, which accounts for the 80% inhibition of the luciferase refolding activity.

In summary, KU675, a novel C-terminal Hsp90 inhibitor, exhibits potent anti-proliferative and cytotoxic activity along with client protein degradation, without induction of the heat shock response (HSR) in both androgen-dependent and -independent prostate cancer cell lines. KU675 displays preferential inhibition of the Hsp90 $\alpha$  isoform, and at the same time, KU675 also inhibits Hsc70. The presented data suggests the potential to design isoform selective inhibitors of Hsp90 as well as, dual inhibitors of other heat shock proteins for the treatment of cancer.

## **Acknowledgements**

The authors would like to thank Dr. Aron W. Fenton at the Department of Biochemistry and Molecular Biology, University of Kansas Medical Center for providing the SPECTRAmax M5 Spectrophotometer. We also extend special thanks to Dr. Russ Middaugh at the Department of Pharmaceutical Chemistry, The University of Kansas for invaluable scientific input in the drug binding study.

## **Authorship Contributions**

Participated in research design: Liu, Vielhauer, Holzbeierlein, and Blagg

Conducted experiments: Liu, Brown, and Ghosh

Contributed new reagents or analytic tools: Zhao

Performed data analysis: Liu, Brown, and Ghosh

Wrote or contributed to the writing of the manuscript: Liu, Holzbeierlein, Lee, and Blagg

## References

- An WG, Schulte TW and Neckers LM (2000) The heat shock protein 90 antagonist geldanamycin alters chaperone association with p210bcr-abl and v-src proteins before their degradation by the proteasome. *Cell growth & differentiation : the molecular biology journal of the American Association for Cancer Research* **11**(7): 355-360.
- Avila C, Hadden MK, Ma Z, Kornilayev BA, Ye QZ and Blagg BS (2006) High-throughput screening for Hsp90 ATPase inhibitors. *Bioorganic & medicinal chemistry letters* **16**(11): 3005-3008.
- Ayala G, Thompson T, Yang G, Frolov A, Li R, Scardino P, Ohori M, Wheeler T and Harper W (2004) High levels of phosphorylated form of Akt-1 in prostate cancer and non-neoplastic prostate tissues are strong predictors of biochemical recurrence. *Clinical cancer research : an official journal of the American Association for Cancer Research* **10**(19): 6572-6578.
- Basso AD, Solit DB, Munster PN and Rosen N (2002) Ansamycin antibiotics inhibit Akt activation and cyclin D expression in breast cancer cells that overexpress HER2. *Oncogene* **21**(8): 1159-1166.
- Blagosklonny MV, Toretsky J and Neckers L (1995) Geldanamycin selectively destabilizes and conformationally alters mutated p53. *Oncogene* **11**(5): 933-939.

Burlison JA, Avila C, Vielhauer G, Lubbers DJ, Holzbeierlein J and Blagg BS (2008)

Development of novobiocin analogues that manifest anti-proliferative activity against several cancer cell lines. *The Journal of organic chemistry* **73**(6): 2130-2137.

Chen B, Piel WH, Gui L, Bruford E and Monteiro A (2005) The HSP90 family of genes in the human genome: insights into their divergence and evolution. *Genomics* **86**(6): 627-637.

Chen B, Zhong D and Monteiro A (2006) Comparative genomics and evolution of the HSP90 family of genes across all kingdoms of organisms. *BMC genomics* **7**: 156.

Chi KN, Hotte SJ, Yu EY, Tu D, Eigl BJ, Tannock I, Saad F, North S, Powers J, Gleave ME and Eisenhauer EA (2010) Randomized phase II study of docetaxel and prednisone with or without OGX-011 in patients with metastatic castration-resistant prostate cancer. *Journal of clinical oncology : official journal of the American Society of Clinical Oncology* **28**(27): 4247-4254.

Chiosis G, Huezo H, Rosen N, Mimnaugh E, Whitesell L and Neckers L (2003) 17AAG: low target binding affinity and potent cell activity--finding an explanation. *Molecular cancer therapeutics* **2**(2): 123-129.

Csermely P, Schnaider T, Soti C, Prohaszka Z and Nardai G (1998) The 90-kDa molecular chaperone family: structure, function, and clinical applications. A comprehensive review. *Pharmacology & therapeutics* **79**(2): 129-168.

Eskew JD, Sadikot T, Morales P, Duren A, Dunwiddie I, Swink M, Zhang X, Hembruff S, Donnelly A, Rajewski RA, Blagg BS, Manjarrez JR, Matts RL, Holzbeierlein JM and Vielhauer GA (2011) Development and characterization of a novel C-terminal inhibitor

of Hsp90 in androgen dependent and independent prostate cancer cells. *BMC cancer* **11**: 468.

Hanahan D and Weinberg RA (2000) The hallmarks of cancer. *Cell* **100**(1): 57-70.

Holzbeierlein JM, Windsperger A and Vielhauer G (2010) Hsp90: a drug target? *Current oncology reports* **12**(2): 95-101.

Huggins C (1952) Endocrine factors in cancer. *The Journal of urology* **68**(6): 875-884.

Huggins C and Hodges CV (2002) Studies on prostatic cancer: I. The effect of castration, of estrogen and of androgen injection on serum phosphatases in metastatic carcinoma of the prostate. 1941. *The Journal of urology* **168**(1): 9-12.

Isaacs JS, Xu W and Neckers L (2003) Heat shock protein 90 as a molecular target for cancer therapeutics. *Cancer cell* **3**(3): 213-217.

Kelly WK, Halabi S, Carducci M, George D, Mahoney JF, Stadler WM, Morris M, Kantoff P, Monk JP, Kaplan E, Vogelzang NJ and Small EJ (2012) Randomized, double-blind, placebo-controlled phase III trial comparing docetaxel and prednisone with or without bevacizumab in men with metastatic castration-resistant prostate cancer: CALGB 90401. *Journal of clinical oncology : official journal of the American Society of Clinical Oncology* **30**(13): 1534-1540.

Kleeberger W, Bova GS, Nielsen ME, Herawi M, Chuang AY, Epstein JI and Berman DM (2007) Roles for the stem cell associated intermediate filament Nestin in prostate cancer migration and metastasis. *Cancer research* **67**(19): 9199-9206.

- Kusuma BR, Khandelwal A, Gu W, Brown D, Liu W, Vielhauer G, Holzbeierlein J and Blagg BS (2014) Synthesis and biological evaluation of coumarin replacements of novobiocin as Hsp90 inhibitors. *Bioorganic & medicinal chemistry* **22**(4): 1441-1449.
- Lassi K and Dawson NA (2010) Update on castrate-resistant prostate cancer: 2010. *Current opinion in oncology* **22**(3): 263-267.
- Marcu MG, Chadli A, Bouhouche I, Catelli M and Neckers LM (2000) The heat shock protein 90 antagonist novobiocin interacts with a previously unrecognized ATP-binding domain in the carboxyl terminus of the chaperone. *The Journal of biological chemistry* **275**(47): 37181-37186.
- Martin CJ, Gaisser S, Challis IR, Carletti I, Wilkinson B, Gregory M, Prodromou C, Roe SM, Pearl LH, Boyd SM and Zhang MQ (2008) Molecular characterization of macbecin as an Hsp90 inhibitor. *Journal of medicinal chemistry* **51**(9): 2853-2857.
- Matthews SB, Vielhauer GA, Manthe CA, Chaguturu VK, Szabla K, Matts RL, Donnelly AC, Blagg BS and Holzbeierlein JM (2010) Characterization of a novel novobiocin analogue as a putative C-terminal inhibitor of heat shock protein 90 in prostate cancer cells. *The Prostate* **70**(1): 27-36.
- Mohler JL (2008) A role for the androgen-receptor in clinically localized and advanced prostate cancer. *Best practice & research Clinical endocrinology & metabolism* **22**(2): 357-372.
- Ohba S, Hirose Y, Yoshida K, Yazaki T and Kawase T (2010) Inhibition of 90-kD heat shock protein potentiates the cytotoxicity of chemotherapeutic agents in human glioma cells. *Journal of neurosurgery* **112**(1): 33-42.



- Peterson LB, Eskew JD, Vielhauer GA and Blagg BS (2012) The hERG channel is dependent upon the Hsp90alpha isoform for maturation and trafficking. *Molecular pharmaceutics* **9**(6): 1841-1846.
- Petrylak DP, Tangen CM, Hussain MH, Lara PN, Jr., Jones JA, Taplin ME, Burch PA, Berry D, Moinpour C, Kohli M, Benson MC, Small EJ, Raghavan D and Crawford ED (2004) Docetaxel and estramustine compared with mitoxantrone and prednisone for advanced refractory prostate cancer. *The New England journal of medicine* **351**(15): 1513-1520.
- Pettaway CA, Pathak S, Greene G, Ramirez E, Wilson MR, Killion JJ and Fidler IJ (1996) Selection of highly metastatic variants of different human prostatic carcinomas using orthotopic implantation in nude mice. *Clinical cancer research : an official journal of the American Association for Cancer Research* **2**(9): 1627-1636.
- Powers MV and Workman P (2007) Inhibitors of the heat shock response: biology and pharmacology. *FEBS letters* **581**(19): 3758-3769.
- Qin H, Hu J, Hua Y, Challa SV, Cross TA and Gao FP (2008) Construction of a series of vectors for high throughput cloning and expression screening of membrane proteins from *Mycobacterium tuberculosis*. *BMC biotechnology* **8**: 51.
- Roe SM, Prodromou C, O'Brien R, Ladbury JE, Piper PW and Pearl LH (1999) Structural basis for inhibition of the Hsp90 molecular chaperone by the antitumor antibiotics radicicol and geldanamycin. *Journal of medicinal chemistry* **42**(2): 260-266.
- Sadikot T, Swink M, Eskew JD, Brown D, Zhao H, Kusuma BR, Rajewski RA, Blagg BS, Matts RL, Holzbeierlein JM and Vielhauer GA (2013) Development of a high-throughput

screening cancer cell-based luciferase refolding assay for identifying Hsp90 inhibitors.

*Assay and drug development technologies* **11**(8): 478-488.

Sato S, Fujita N and Tsuruo T (2000) Modulation of Akt kinase activity by binding to Hsp90.

*Proceedings of the National Academy of Sciences of the United States of America* **97**(20): 10832-10837.

Schulte TW, Blagosklonny MV, Ingui C and Neckers L (1995) Disruption of the Raf-1-Hsp90 molecular complex results in destabilization of Raf-1 and loss of Raf-1-Ras association.

*The Journal of biological chemistry* **270**(41): 24585-24588.

Schulte TW and Neckers LM (1998) The benzoquinone ansamycin 17-allylamino-17-

demethoxygeldanamycin binds to HSP90 and shares important biologic activities with geldanamycin. *Cancer chemotherapy and pharmacology* **42**(4): 273-279.

Shelton SN, Shawgo ME, Matthews SB, Lu Y, Donnelly AC, Szabla K, Tanol M, Vielhauer

GA, Rajewski RA, Matts RL, Blagg BS and Robertson JD (2009) KU135, a novel novobiocin-derived C-terminal inhibitor of the 90-kDa heat shock protein, exerts potent antiproliferative effects in human leukemic cells. *Molecular pharmacology* **76**(6): 1314-1322.

Siegel R, Ward E, Brawley O and Jemal A (2011) Cancer statistics, 2011: the impact of

eliminating socioeconomic and racial disparities on premature cancer deaths. *CA: a cancer journal for clinicians* **61**(4): 212-236.

Sreedhar AS, Kalmar E, Csermely P and Shen YF (2004) Hsp90 isoforms: functions,

expression and clinical importance. *FEBS letters* **562**(1-3): 11-15.

- Stuhmer T, Chatterjee M, Grella E, Seggewiss R, Langer C, Muller S, Schoepfer J, Garcia-Echeverria C, Quadt C, Jensen MR, Einsele H and Bargou RC (2009) Anti-myeloma activity of the novel 2-aminothienopyrimidine Hsp90 inhibitor NVP-BEP800. *British journal of haematology* **147**(3): 319-327.
- Suda A, Kawasaki K, Komiyama S, Isshiki Y, Yoon DO, Kim SJ, Na YJ, Hasegawa K, Fukami TA, Sato S, Miura T, Ono N, Yamazaki T, Saitoh R, Shimma N, Shiratori Y and Tsukuda T (2014) Design and synthesis of 2-amino-6-(1H,3H-benzo[de]isochromen-6-yl)-1,3,5-triazines as novel Hsp90 inhibitors. *Bioorganic & medicinal chemistry* **22**(2): 892-905.
- Tannock IF, de Wit R, Berry WR, Horti J, Pluzanska A, Chi KN, Oudard S, Theodore C, James ND, Turesson I, Rosenthal MA, Eisenberger MA and Investigators TAX (2004) Docetaxel plus prednisone or mitoxantrone plus prednisone for advanced prostate cancer. *The New England journal of medicine* **351**(15): 1502-1512.
- Thulasiraman V and Matts RL (1996) Effect of geldanamycin on the kinetics of chaperone-mediated renaturation of firefly luciferase in rabbit reticulocyte lysate. *Biochemistry* **35**(41): 13443-13450.
- Thulasiraman V and Matts RL (1998) Luciferase renaturation assays of chaperones and chaperone antagonists. *Methods in molecular biology* **102**: 129-141.
- Whitesell L and Lindquist SL (2005) HSP90 and the chaperoning of cancer. *Nature reviews Cancer* **5**(10): 761-772.
- Xu W, Mimnaugh E, Rosser MF, Nicchitta C, Marcu M, Yarden Y and Neckers L (2001) Sensitivity of mature ErbB2 to geldanamycin is conferred by its kinase domain and is

mediated by the chaperone protein Hsp90. *The Journal of biological chemistry* **276**(5): 3702-3708.

Zhang H and Burrows F (2004) Targeting multiple signal transduction pathways through inhibition of Hsp90. *Journal of molecular medicine* **82**(8): 488-499.

## Footnotes

This work was supported by the National Institutes of Health [Grant CA120458].

## Legends for Figures

### Figure 1.

**KU675, a novel analog of novobiocin, causes anti-proliferative effects in prostate cancer cells.**

(A) The structures of novobiocin and KU675. PC3MM2 (B), LNCap-LN3 (C), LAPC-4 (D) and C4-2 (E) cells were cultured in a 96-well white plate with corresponding medium, and treated with KU675 for 24 hr (●) and 48 hr (■). Cell Titer-Glo® Luminescent reagent was used to measure cellular proliferation. Data were analyzed from three independent experiments performed in triplicate; each data point represents the mean  $\pm$  SEM.

### Figure 2.

**Cytotoxicity of KU675 in prostate cancer cells.**

LNCap-LN3 (A), LAPC-4 (B), C4-2 cells (C) were treated with KU675 for 24 hr, and PC3MM2 cells were treated for both 24 hr (D) and 48 hr (E). Samples were mixed with equal parts Trypan Blue and assessed for viability by Vi-Cell™ Cell Viability Analyzer. Percentage viability was calculated as described in Materials and Methods Section. Columns depict the mean  $\pm$  SEM from three independent experiments (n=3). Asterisks \*, \*\*, and \*\*\* indicates

significant P value < 0.05, < 0.01, and < 0.001, respectively, by two-tailed t-test compared to vehicle-treated (DMSO) control.

### **Figure 3.**

#### **Cancer cell based Hsp90 dependent luciferase refolding assay.**

Inhibition of luciferase refolding in PC3MM2 (A) and LNCap-LN3 (B) cancer cells in dose response with N-terminal (17AAG) and C-terminal Hsp90 (KU675) inhibitors was measured at 60 minute time points. Luciferase activity is reported as a percentage of its control activity for each drug concentration. These results are the mean  $\pm$  SEM from three independent experiments performed in duplicate (n=3).

### **Figure 4.**

#### **KU675 mediated client protein degradation in the absence of heat shock protein induction.**

PC3MM2 (A), LNCap-LN3 (B), LAPC-4 (C), and C4-2 cells (D) were examined for client protein degradation and the induction of heat shock proteins. 17-AAG demonstrates Hsp induction in all four cancer cell lines while KU675 triggers a dose-dependent decrease in several client proteins known to play a role in the etiology of prostate cancer. (E) Western blots were run with the wild type, Hsp90 $\alpha$ , and Hsp90 $\beta$  knock down PC3MM2 cell lines and blotted

against Hsp90 $\alpha$ , Akt, pAkt (S473), pAkt (T308), Cyclin D1, Survivin, c-Src, Raf, Erk5, Hsp90 $\beta$ , CXCR4. Actin was used as loading control.

### Figure 5.

#### **Analysis of the binding of KU675 to Hsp90 exhibits isoform selectivity for Hsp90 $\alpha$ .**

Intrinsic fluorescence spectra were used to test the specific binding of KU675 to Hsp90. KU675 (20  $\mu$ M) was incubated with Hsp90 $\alpha$  (A), Hsp90 $\beta$  (B), and a negative control protein PhK (C) at different concentrations: 0 to 100  $\mu$ g/mL for Hsp90 $\alpha$ , 0 to 140  $\mu$ g/mL for Hsp90 $\beta$ , and 0 to 100  $\mu$ g/mL for PhK. After 30 mins, KU675 (20  $\mu$ M) was excited at 345nm, and the emission peak was monitored from 350 to 600nm. Concentration dependent binding curves for the interaction of KU675 with Hsp90 $\alpha$  and  $\beta$  were generated using the non-linear regression of the data with Scatchard plot inserted. Dose-dependent effects of KU675 on Hsp90 $\alpha$  and Hsp90 $\beta$  native complexes were determined by Blue Native western blot after treatment of PC3MM2 cells by KU675 along with 17-AAG and novobiocin (D), protein concentration was determined using DC Protein Assay to ensure equal amounts of protein were loaded and a loading control  $\beta$ -actin was included in each experiment. Hsp90 $\alpha$  complex was significantly disrupted by KU675, while Hsp90 $\beta$  complex only showed moderate change.

### Figure 6.

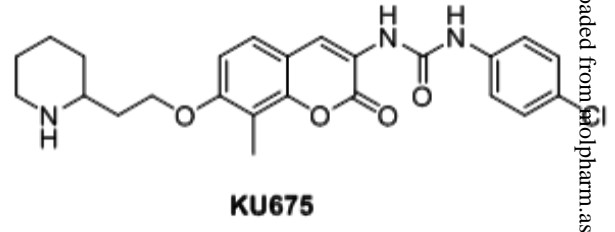
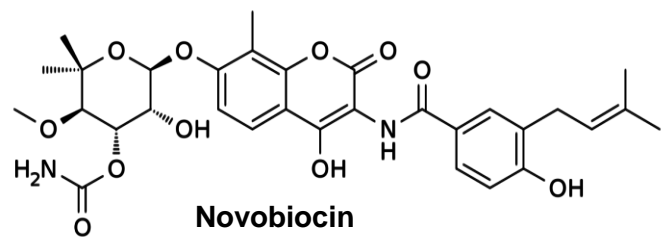
#### **KU675 binds to Hsc70 and decreases the expression levels of HSC70 client proteins.**

Fig. 6A demonstrates the intrinsic fluorescence spectra of 20  $\mu$ M KU675 in the presence of Hsp90 $\alpha$ ,  $\beta$  and Hsc70, while Fig. 6B displays replot of relative fluorescence intensity versus concentration of Hsc70 ( 0 to 30  $\mu$ g/mL) with a Scatchard plot inserted. Fig. 6C shows the decreased expression of Hsc70 specific client proteins induced by KU675.

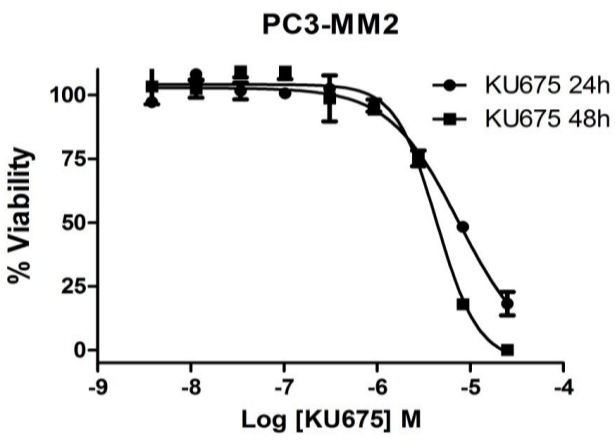


Figure 1

**A**

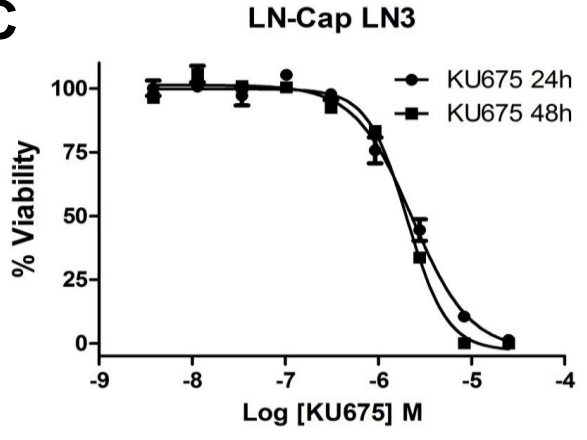


**B**



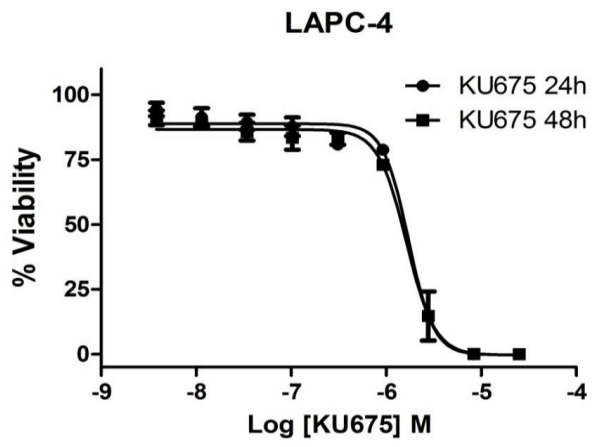
	KU675 24h	KU675 48h
IC50	7.508e-006	4.396e-006

**C**



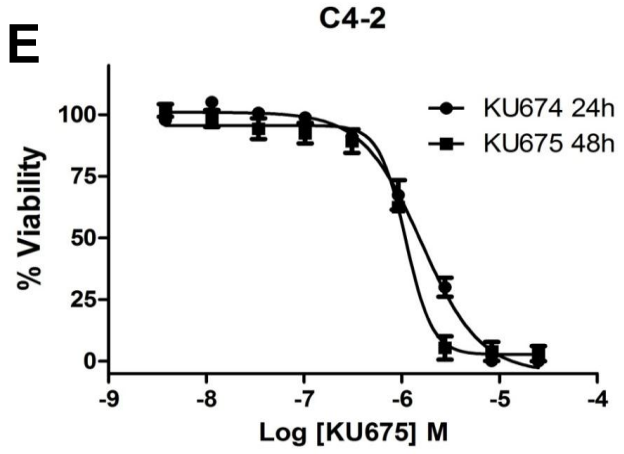
	KU675 24h	KU675 48h
IC50	2.303e-006	2.048e-006

**D**



	KU675 24h	KU675 48h
IC50	1.711e-006	1.634e-006

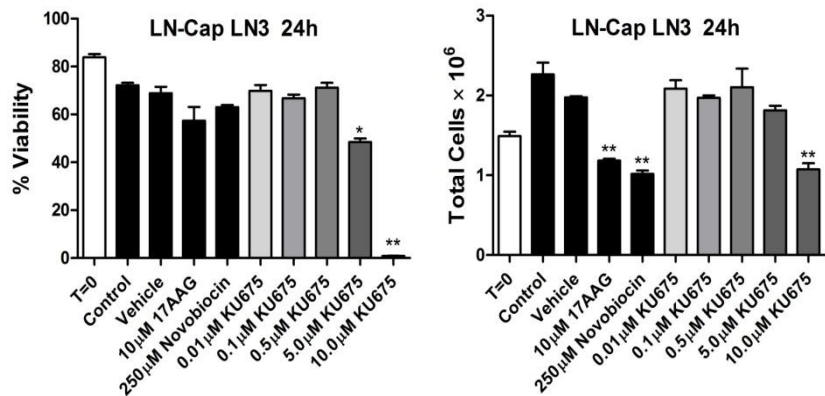
**E**



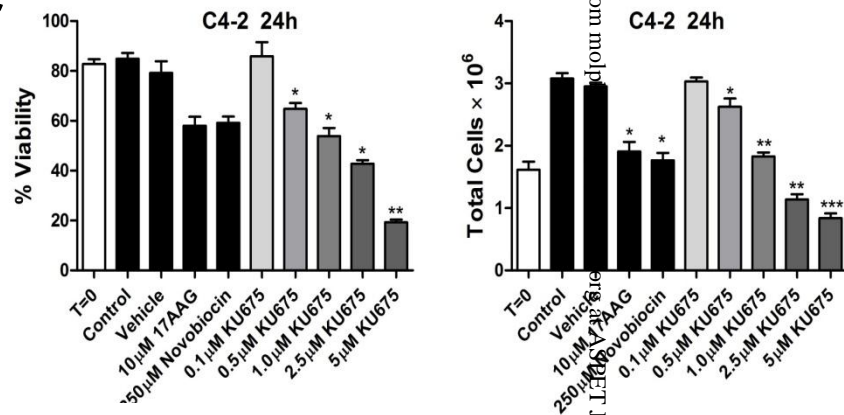
	KU675 24h	KU675 48h
IC50	1.589e-006	1.101e-006

Figure 2

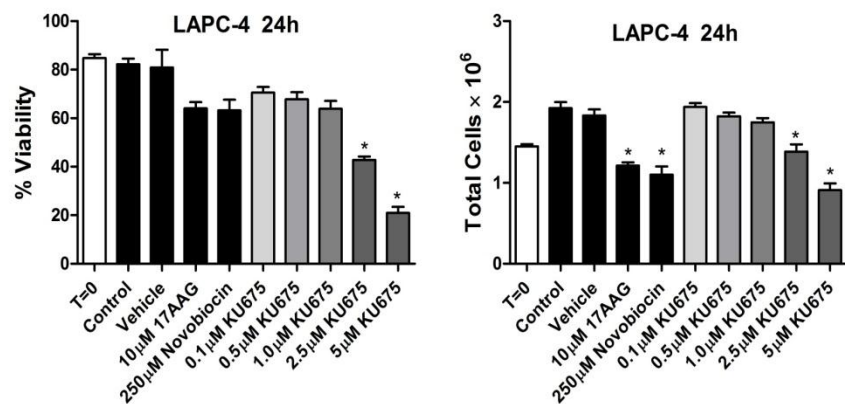
**A**



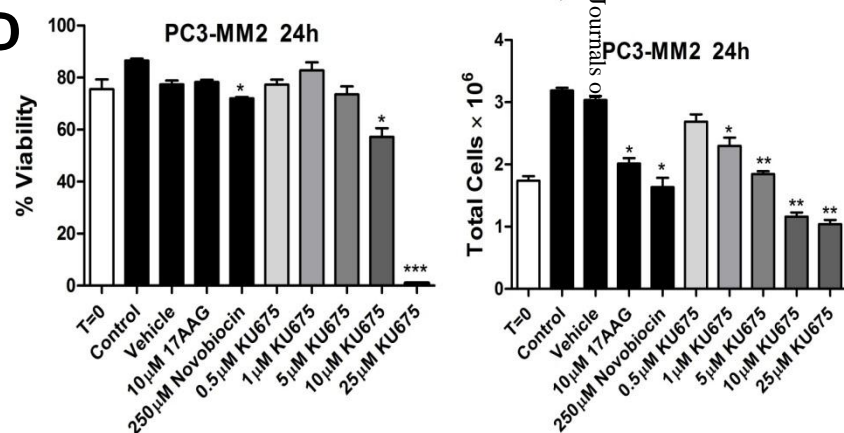
**C**



**B**



**D**



**E**

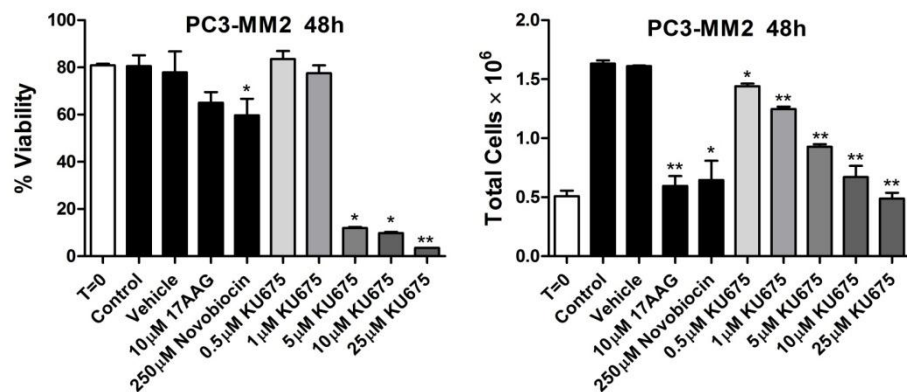
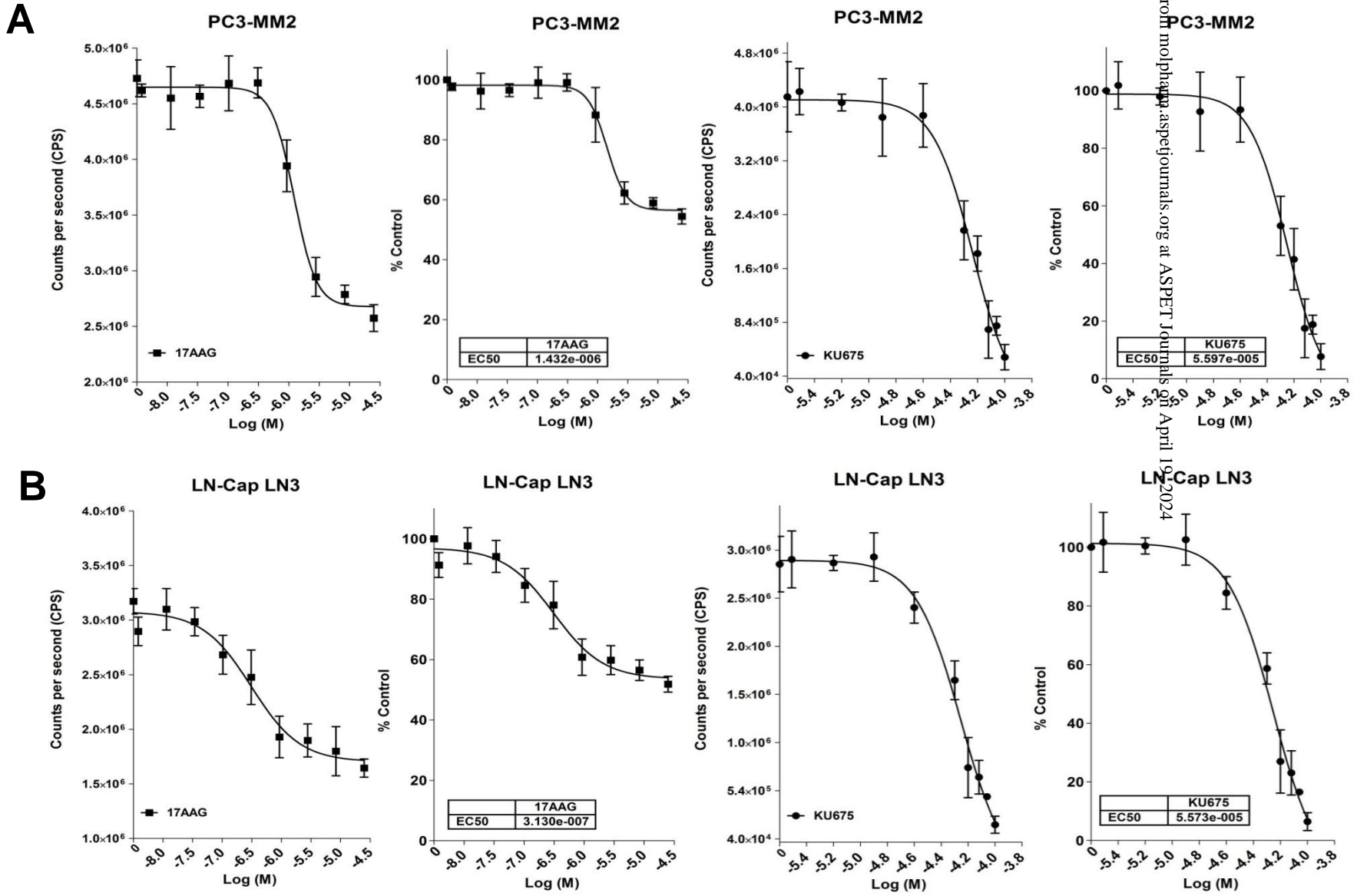


Figure 3



Downloaded from [molpharm.aspetjournals.org](http://molpharm.aspetjournals.org) at ASPET Journals on April 19, 2024

Figure 4

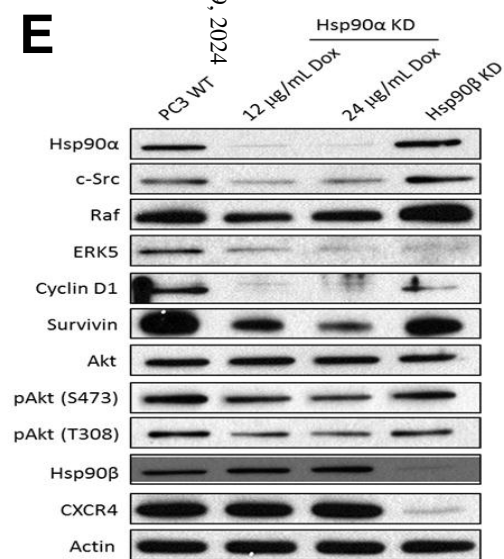
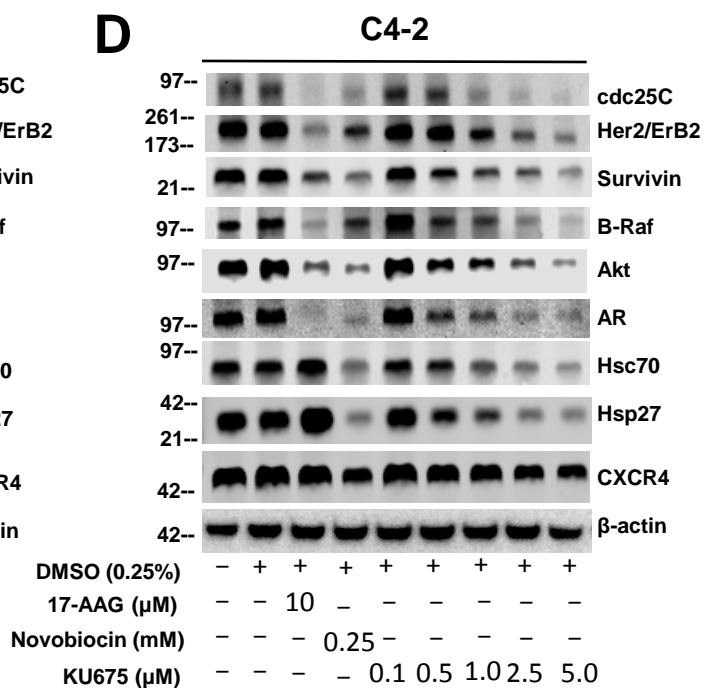
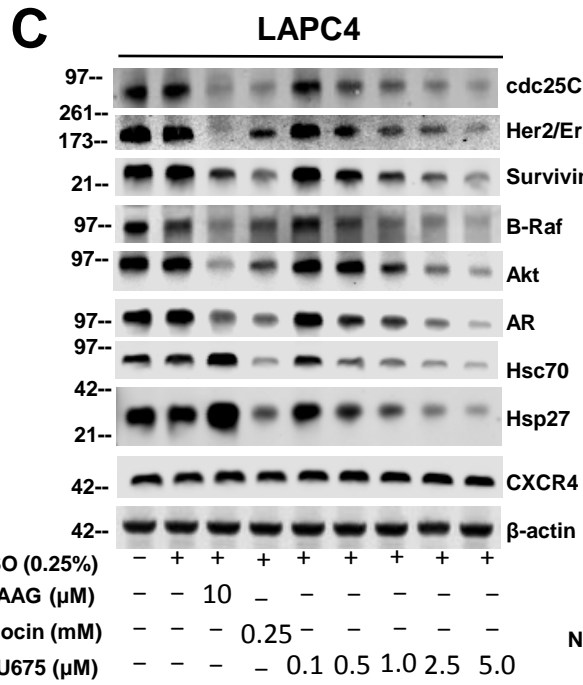
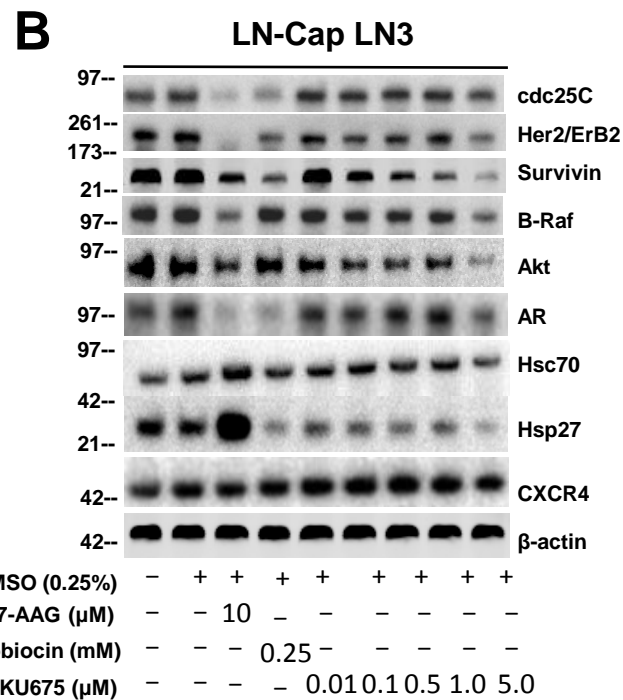
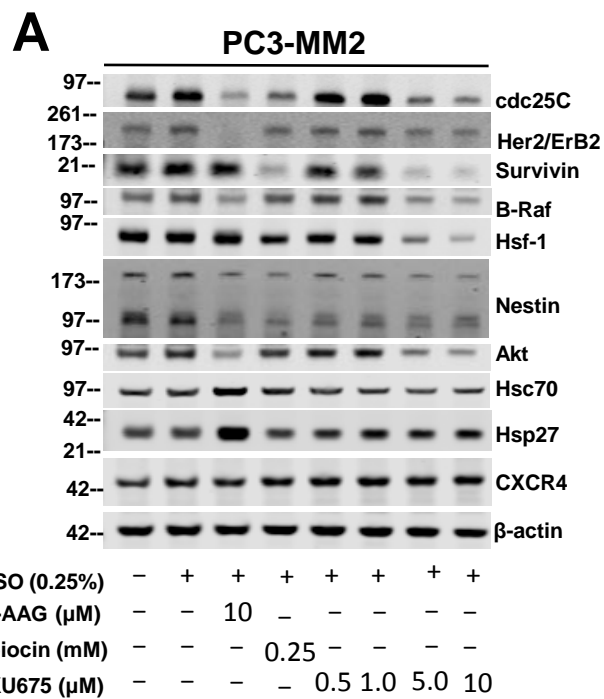
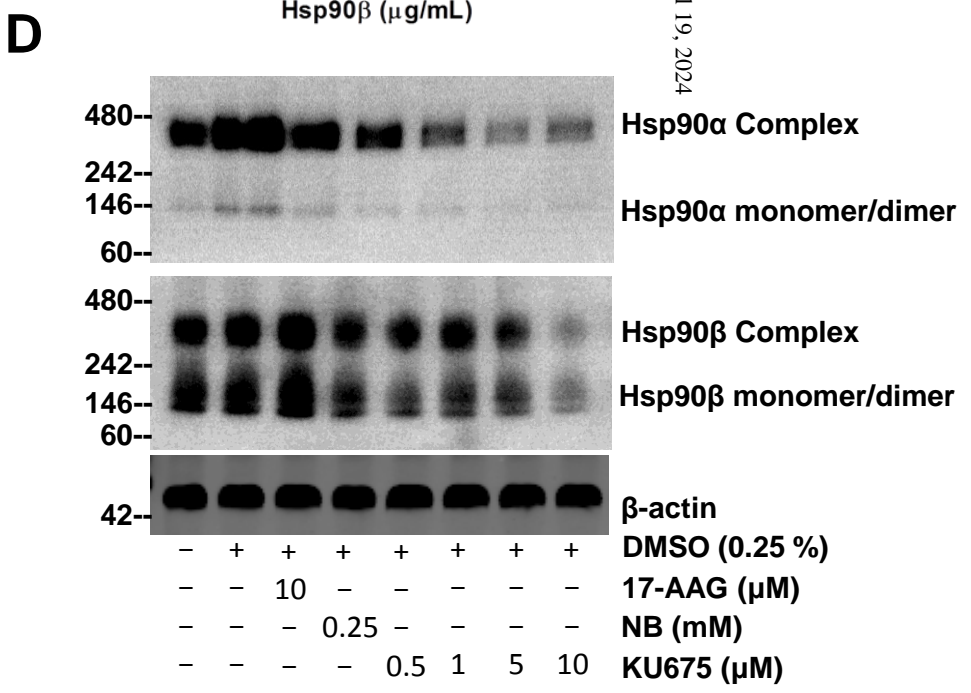
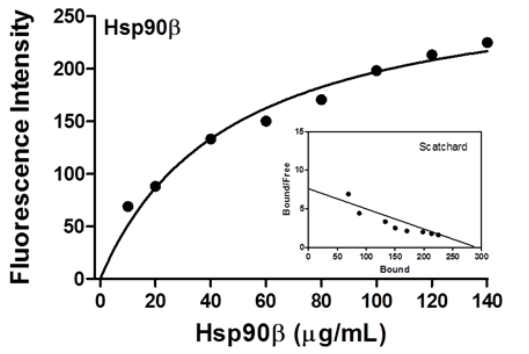
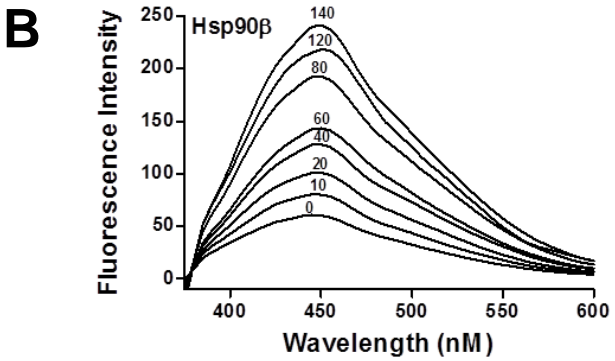
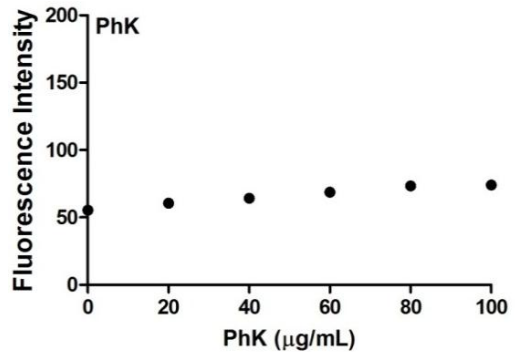
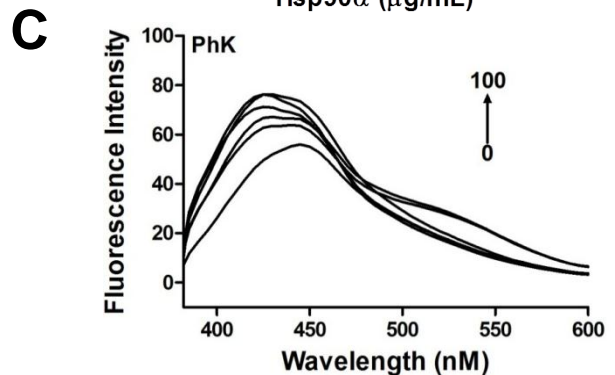
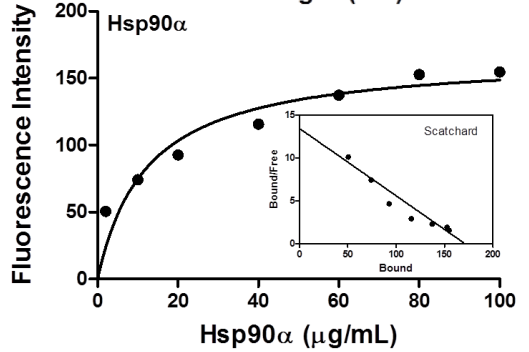
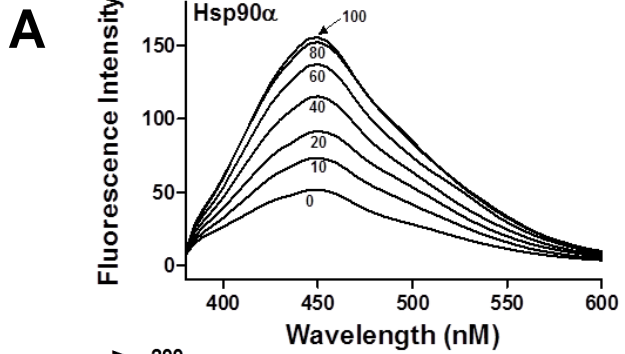
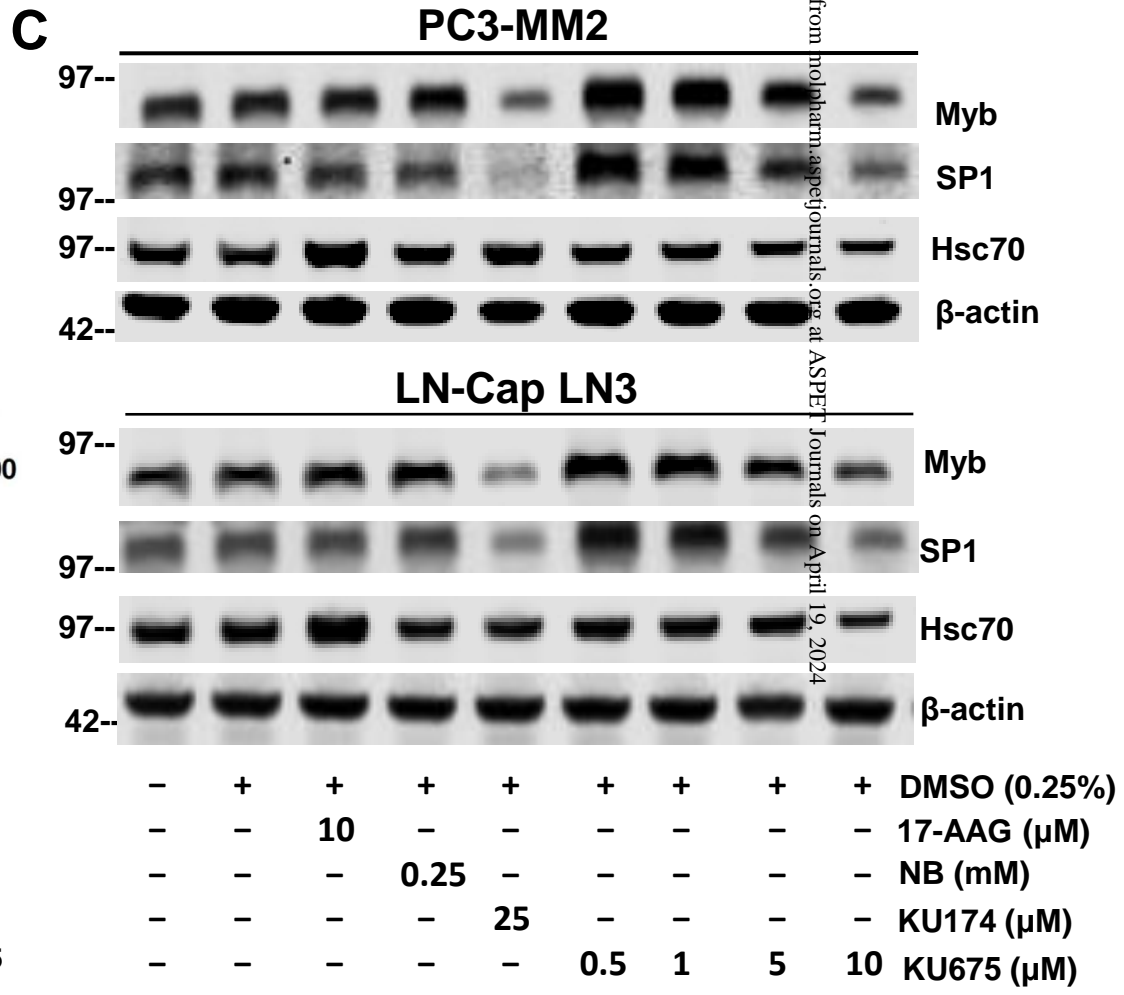
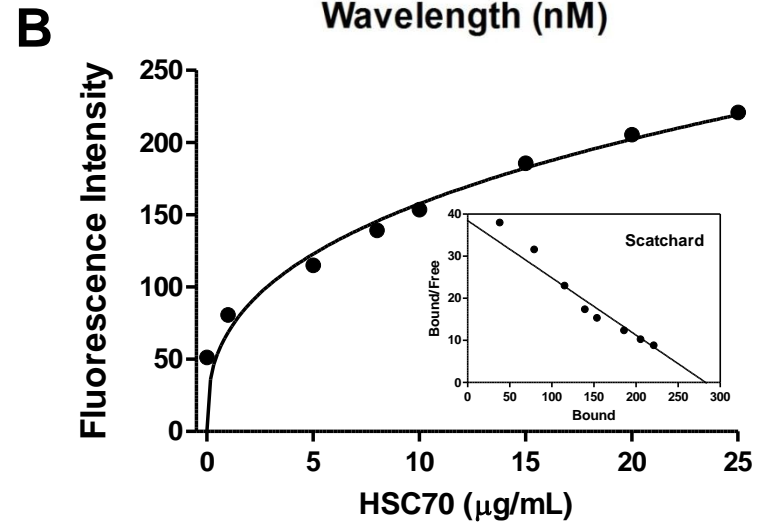
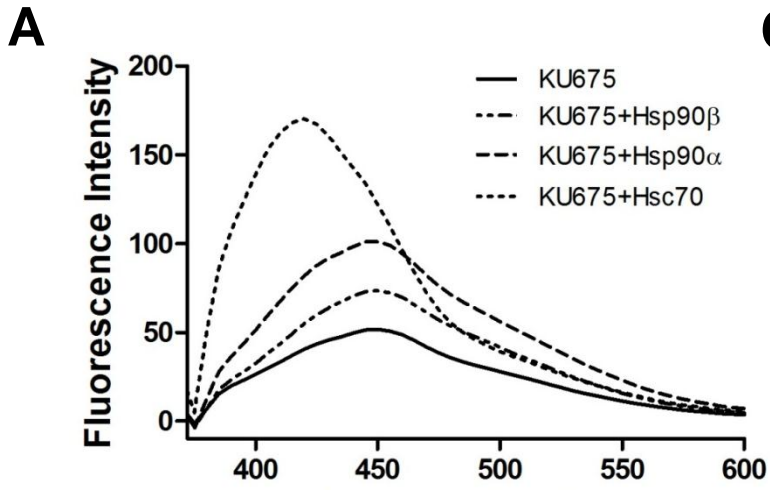


Figure 5



Downloaded from molpharm.aspetjournals.org at ASPET Journals on April 19, 2024

Figure 6



Downloaded from https://pubs.ascpjournals.org/ at ASPET Journals on April 19, 2024